Available online at www.sciencedirect.com

ScienceDirect

Geochimica et Cosmochimica Acta 220 (2018) 110–124

Geochimica et Cosmochimica Acta

www.elsevier.com/locate/gca

Position-specific ^{13}C distributions within propane from experiments and natural gas samples

Alison Piasecki [a,*], Alex Sessions [a], Michael Lawson [b], A.A. Ferreira [c], E.V. Santos Neto [c], Geoffrey S. Ellis [d], Michael D. Lewan [d], John M. Eiler [a]

[a] Division of Geological and Planetary Sciences, California Institute of Technology, Pasadena, CA 91125, USA
[b] Exxon Mobil Upstream Research Company, Spring, TX 77389, USA
[c] Division of Geochemistry, PETROBRAS Research and Development Center (CENPES), PETROBRAS, Rua Horácio Macedo, 950, Ilha do Fundão, Rio de Janeiro, RJ 21941-915, Brazil
[d] U.S. Geological Survey, Central Energy Resources Science Center, P.O. Box 25046, Denver Federal Center, Denver, CO 80225, USA

Received 30 January 2017; accepted in revised form 24 September 2017; available online 6 October 2017

Abstract

Site-specific carbon isotope measurements of organic compounds potentially recover information that is lost in a conventional, 'bulk' isotopic analysis. Such measurements are useful because isotopically fractionating processes may have distinct effects at different molecular sites, and thermodynamically equilibrated populations of molecules tend to concentrate heavy isotopes in one molecular site versus another. Most recent studies of site-specific ^{13}C in organics use specialized Nuclear Magnetic Resonance (NMR) techniques or complex chemical degradations prior to mass spectrometric measurements. Herein we present the first application of a new mass spectrometric technique that reconstructs the site-specific carbon isotope composition of propane based on measurements of the $^{13}C/^{12}C$ ratios of two or more fragment ions that sample different proportions of the terminal and central carbon sites. We apply this method to propane from laboratory experiments and natural gas samples to explore the relationships between site-specific carbon isotope composition, full-molecular $\delta^{13}C$, thermal maturity, and variation in organic matter precursors. Our goal is to advance the understanding of the sources and histories of short-chain alkanes within geologic systems. Our findings suggest that propane varies in its site-specific carbon isotope structure, which is correlated with increasing thermal maturity, first increasing in terminal position $\delta^{13}C$ and then increasing in both center and terminal position $\delta^{13}C$. This pattern is observed in both experimental and natural samples, and is plausibly explained by a combination of site-specific, temperature-dependent isotope effects associated with conversion of different precursor molecules (kerogen, bitumen, and/or oil) to propane, differences in site-specific isotopic contents of those precursors, and possibly distillation of reactive components of those precursors with increasing maturity. We hypothesize that the largest changes in site-specific isotopic content of propane occur when bitumen and/or oil replace kerogen as the dominant precursors. If correct, this phenomenon could have significant utility for understanding gas generation in thermogenic petroleum systems.

Keywords: Isotope geochemistry; Site-specific isotopes

1. INTRODUCTION

Stable isotopes are useful tracers in natural gas systems, as they are sensitive to differences in source compositions (e.g., marine vs. lacustrine source rocks), often vary system-

* Corresponding author at: University of Bergen, Earth Science Department, Postboks 7803, 5020 Bergen, Norway.
E-mail address: piasecki@gps.caltech.edu (A. Piasecki).

https://doi.org/10.1016/j.gca.2017.09.042
0016-7037/

atically with source rock and fluid thermal maturity, type and extent of any alteration processes that impact fluid composition, and may be used as a tracer of mixing between different reservoirs (Chung and Sackett, 1979; Tang et al., 2005; Schimmelmann and Sessions, 2006). However, many natural gases are simultaneously influenced by several of these factors, leading to $\delta^{13}C$ values (either for bulk gas or specific compounds) that have non-unique interpretations. Differences in $\delta^{13}C$ between coexisting compounds (i.e., methane, ethane and propane) combined with abundance patterns may help deconvolve the various confounding influences (Chung et al., 1988), nevertheless it remains true that the stable isotope compositions of natural hydrocarbons are in many cases ambiguous (Zou et al., 2007). Herein, we present the results of a recently developed method for site-specific carbon isotope analysis of propane (Piasecki et al., 2016a), which adds additional isotopic constraints to help distinguish the various source histories of natural gases. Recent studies report site-specific C isotope compositions of various commercially available long-chain *n*-alkanes (Gilbert et al., 2013) as well as a few propane samples (Gilbert et al., 2016; Gao et al., 2016; Suda et al., 2017). However, to the best of our knowledge, this is the first systematic study of the C isotope structures of alkanes having well-constrained synthetic or natural origins, and thus may serve as an example for future studies of larger organic molecules.

2. BACKGROUND

2.1. The carbon isotope structures of organic molecules

It has long been suggested that the biologic synthesis of molecules like amino acids and fatty acids should lead to site-specific isotope patterns that depend on their particular biosynthetic pathways. For example, the cleavage of pyruvate leads to a difference in $\delta^{13}C$ between the methyl and C═O carbons in product acetyl groups, an effect that was predicted to be somehow incorporated within fatty acids (DeNiro and Epstein, 1977). The explicit even-odd ordering of carbon isotopes was proposed and then confirmed by direct measurements of site-specific carbon isotope variations in natural fatty acids using selective chemical decompositions (Monson and Hayes, 1980, 1982). Broadly similar (although less well-understood) metabolic kinetic isotope effects are responsible for site-specific carbon isotope variations in amino acids (Abelson and Hoering, 1961), and contribute to differences in $\delta^{13}C$ between different amino acids (Macko et al., 1987). It has also been predicted from first-principles theory that equilibrium thermodynamic driving forces should tend to promote intra- and intermolecular differences in $\delta^{13}C$ of amino acids, broadly resembling those observed in biological samples (Rustad, 2009).

Recent advances in NMR analysis of natural isotope distributions (2H NMR) have substantially expanded the range of site-specific isotope effects that have been measured and the classes of compounds in which they can be observed. These methods have been used to quantify proportions of deuterium isotopologues of cellulose (Betson et al., 2006), oxygen and carbon fractionations in cellulose (Guy et al., 1993), and vanillin (Caer et al., 1991), among other compounds. NMR is currently the best means available for observing the diversity of site-specific isotope effects in common, abundant organic compounds that can be isolated in substantial quantity (100 s of mg). However, it will be very challenging to apply site specific natural isotopic fractionation (SNIF)-NMR methods to sample sizes more typical of environmental samples (μg to mg) (Gilbert et al., 2012). Herein, we apply a recently developed method that uses the characteristic fragmentation spectrum created during electron-impact ionization to probe the isotopic enrichment of different parts of a molecule, where the fragments are analyzed for their isotopic proportions using high-resolution gas source mass spectrometry (Piasecki et al., 2016a). We use this technique to explore the site-specific ^{13}C signatures associated with the competing factors that govern the bulk isotopic content of propane.

2.2. Geologic background of measured samples

We measured a variety of different types of samples within this study from experimental to natural samples generated in a wide range of geologic settings. Since the method of generation determines the stable isotope structure, it is necessary to consider the history of the samples, which is discussed in the following sections.

2.2.1. Hydrous pyrolysis experiments

Hydrous pyrolysis experiments were conducted in the Energy Geochemistry Laboratories of the U.S. Geological Survey in Denver, CO, following the methods of Lewan (1997) using Woodford Shale as starting material (Lewan, 1997). Information pertaining to the characteristics of this organic-rich source rock can be found in Lewan (1983) and subsequent studies (Lewan, 1985, 1993, 1997). Rock powders were heated with water in a closed system for 72 h each at four temperatures: 330, 360, 390 and 415 °C to simulate different stages of maturation of source rocks. The experiments were conducted sequentially, such that, at the end of the first 72-h heating period the reactor was cooled to room temperature, the generated gases recovered, small aliquots of generated oil and residual rock were removed, and the reactor was then resealed and heated to the next higher temperature.

2.2.2. Potiguar Basin, Brazil

Next, we chose propane from the onshore portion of the Potiguar Basin in northeastern Brazil. Propane samples were collected in conventional natural petroleum accumulations that produce oil and gas with a range of inferred thermal maturities. All sampled fields derive from the Pendência petroleum system that holds both source and reservoir rocks.

The basin was formed during the Early Cretaceous and its tectonic and stratigraphic evolution can be divided into three main stages: rift, transitional, and drift or oceanic. The rift stage (Neocomian-Barremian) is characterized by lacustrine sediments of the Pendência Formation that have intervals representing an important sequence of source rocks (Morais, 2007). Such source rocks are represented

by gray to black shales interbedded with thin sandstone layers. Total organic carbon (TOC) can reach up to 7 wt%, but generally it averages between 2 and 3 wt%. The hydrocarbon source potential given by Rock-Eval pyrolysis is about 25 kg hydrocarbons/ton rock and low-maturity intervals. The good quality of the organic matter is corroborated by the hydrogen index with values ranging between 600 and 900 mg hydrocarbons/g TOC (Trindade et al., 1992). During the rift stage, tectonism caused intense faulting that produced the characteristic pattern of graben and horst structures (Bertani et al., 1990). The transitional stage (Aptian) is represented by a sequence of carbonates, shales and marls interbedded with deltaic sediments deposited in a restricted, sometimes evaporitic, lagoonal environment with sporadic marine influence (Bertani et al., 1990). Shales and marls were deposited under lacustrine or marine-evaporitic conditions and represent the other important group of source rocks not used in this study. The drift or oceanic stage (Albian to the present) led to the deposition of thick sedimentary sequences under open-marine conditions. One sequence is composed of transgressive shales and shelf carbonates covering fluvial sandstones in a shelf-slope system (Albian-Turonian); the other is a progradational sequence represented by siliciclastic facies, carbonates, pelites and turbidites (Campanian to Holocene). Oils produced in the Potiguar Basin are classified according to their correlative source rocks as either: lacustrine oil (pristane/phytane > 2, gammacerane/C_{30} hopane < 0.4, hopane/sterane > 0.6, $\delta^{13}C_{oil}$ < -29‰, $\delta D_{oil} > -101$‰); marine-evaporitic oil (pristane/phytane < 1, gammacerane/C_{30} hopane > 0.6, hopane/sterane < 0.6, $\delta^{13}C_{oil} > -26.4$‰, $\delta D_{oil} < -114$‰); and mixed oils that share common geochemical features of lacustrine and marine-evaporitic sources (Mello et al., 1988, 1993; Santos Neto dos and Hayes, 1999).

The methane component of the samples analyzed in this study was previously analyzed for clumped isotope thermometry (Stolper et al., 2014a), and the associated ethane was analyzed for its ^{13}C–^{13}C clumped isotope composition (Clog et al., 2013). Herein, we add the site-specific ^{13}C distribution in propane. We evaluated the accuracy of these measurements for this sample suite by comparing the whole-molecule $\delta^{13}C$ value calculated from our measurements of C_1 and C_2 fragment ions to an independently measured $\delta^{13}C$ value determined by gas chromatography – combustion – isotope ratio mass spectrometry (GC-C-IRMS). These conventional measurements were made at the Petrobras Research and Development Center (CENPES). A cross-plot of these two estimates of molecular $\delta^{13}C$ are consistent with a 1:1 slope but an intercept of -0.5‰ (Piasecki et al., 2016a). We attribute this offset to an inter-laboratory difference in standardization. Nevertheless, the correlation between these two independent measurements suggests that our results are accurate (or, at least, that relative differences between samples are accurate).

2.2.3. The Eagle Ford Formation

The Eagle Ford Formation is Late Cretaceous, organic-rich (TOC averages from 2.5 to 5.0 wt%) and contains oil-prone Type IIs kerogen (Hammes et al., 2016; Sun et al., 2016). It has experienced a range in thermal maturities from early oil window through wet and dry gas maturity, across a range of areas in the deposit. Therefore, gas is present as both solution gas and free gas depending on the location of sampling. These are shale gases that extend to relatively low propane contents and high inferred gas maturities; and, they come from an 'unconventional' resource where the gas is inferred to have been stored in its original source rock. This is relevant to potential mechanisms for cracking and isotope exchange, due to the exposure of gases to more abundant catalytic surfaces in shale-hosted deposits.

2.2.4. The Antrim Shale

We examined several samples of propane from the Antrim Shale, located in the Michigan Basin in the Northern US. This is an Upper Devonian black shale, containing 0.5–24 weight percent TOC. It contains Type-II kerogen, and has thermal maturity values on the edges of the basin ranging from 0.4 to 0.6% R_o that increase to 1% in the center of the basin (Martini et al., 2003). At the margins of the basin, groundwater has infiltrated the fractured shale and promoted microbial oxidation of the C_2+ alkanes (including ethane and propane). The primary evidence for this process is the increase in bulk $\delta^{13}C$ values of ethane and propane with decreasing concentration of those species (Martini et al., 2003).

3. METHODS

We measure the site-specific $^{13}C/^{12}C$ ratios of propane using a high-resolution gas source mass spectrometry technique described in Piasecki et al. (2016a); only the key details are summarized here.

3.1. Sample Preparation

Propane is first isolated from other gases (e.g., methane, ethane, butane, CO_2) via a series of vapor-pressure distillation steps using a cryostat. Cryogenically isolated propane is often contaminated by CO_2 due to similarities in their respective vapor pressures. In this case, CO_2 is removed by exposure to ascarite, followed by drierite (to remove water released in the ascarite reaction), followed by a cold trap held at dry ice/ethanol slush temperature to remove any remaining water. A typical sample size of purified propane is approximately 50 μmol. Most of the samples described in this paper have been archived for additional future study.

3.2. Mass spectrometry

Once isolated, propane is introduced into bellows of the MAT-253 Ultra (ThermoFisher Scientific), a high-resolution gas source mass spectrometer (Eiler et al., 2012). Propane has a highly reproducible mass spectrum comprised of 1-, 2- and 3-carbon ions with variable numbers of hydrogens. Piasecki et al. (2016a) established that the 1-carbon ions dominantly sample the terminal carbon

position (C-1 and C-3) of analyte propane, whereas the two-carbon species are equal mixtures of central (C-2) and terminal position carbons (i.e., less than 5% recombination within Piasecki et al. (2016a)). The three-carbon ions sample these carbon positions in their proportions in the full propane molecule (percent level departures from these generalizations occur due to fragmentation/recombination reactions in the ion source and must be corrected for by analysis of isotopically labeled standards). Thus, a measurement of any two ions differing in their carbon numbers, or combination of a measurement of a 1- or 2-carbon piece with a conventional bulk $\delta^{13}C$ value, can be used to solve for the difference in $\delta^{13}C$ between the terminal and central positions.

Ordinarily, we perform sample/standard comparisons of the $^{13}C/^{12}C$ ratios of a one-carbon fragment ion (CH_3^+ or CH_2^+) and a two-carbon fragment ion ($C_2H_4^+$). However, in cases where one or both of these measurements appear to be compromised (see below), we also attempt a measurement of the molecular ion ($C_3H_8^+$; note, this species is measured in such a way that we collect ^{13}C and D isotopomers together, and then ion-correct the combined signal for independently known differences in D/H ratio as described below). Note also that the one-carbon fragment ion population was measured in two different ways over the course of this study: The initial method, which was used for some of the Potiguar Basin samples as well as mixing experiments, involved measuring the ratio of $^{13}CH_3^+/^{12}CH_3^+$. However, nearby isobaric interferences from NH_2 required a background correction that proved to be unstable over time, degrading precision and accuracy. Therefore, we changed our method to look at species one cardinal mass lower, or the ion ratio $^{13}CH_2^+/^{12}CH_2^+$. The two methods were shown to be in agreement when background species were low for both (Piasecki et al., 2016a).

For each measurement, we determine intensities of background ion beams that partially overlap the detector when it is positioned to measure the analyte ion of interest, and their contributions are subtracted. The precision of $^{13}C^{12}CH_4/^{12}C_2H_4$ and $^{13}C^{12}C_2H_8/^{12}C_3H_8$ measurements is 0.1‰, and for the $^{13}CH_2$ measurement is 0.5‰. In cases where the molecular ion has been analyzed along with a small contribution from nearly isobaric $^{12}C_3H_7D$, we recover the sample for separate analysis of the ratio, $^{12}C_3H_7D/^{13}C^{12}C_2H_8$ using a modified Thermo double focusing system (DFS) high-resolution gas source mass spectrometer (Eiler et al., 2014). This is done to remove the contributions of the D-bearing species to the Ultra measurement of the ratio, $[^{12}C_3H_7D + {}^{12}C_2{}^{13}CH_8/^{12}C_3H_8]$, so that the $^{13}C/^{12}C$ ratio of the propane molecule can be evaluated. This procedure may appear complex because it involves multiple stages of analysis, but proved faster and more straightforward than attempting to explicitly mass resolve the ^{13}C and D isotopologues of C_3H_8 on the Ultra. This separation calls for a formal mass resolution of only 15,400. The maximum mass resolution of the Ultra (27,000) exceeds this value, but the large difference in relative abundance between ^{13}C and D means D is barely resolved from the tail of ^{13}C. This problem is not present in the DFS measurement, which cleanly separates the two species.

The primary analytical problem that we encounter is anomalous fractionation behavior in the ion source in the presence of minor contaminants. We have established that the presence of even a small amount of butane in a sample compromises the apparent isotopic composition of the C-1 fragment either by butane contributions to the 1-carbon ion population, or because its presence modifies the instrumental isotopic fractionation associated with ionization and fragmentation of propane. We explain below, in the section titled 'Results,' how we evaluate the accuracy of our results in the face of this problem. In some of the instances where a measurement of the 1- and 2-carbon fragments failed to pass data quality criteria, we attempted a second measurement examining the 2- and 3-carbon ions, which together yield a less precise estimate of the difference in $\delta^{13}C$ between the terminal and central carbon positions simply because neither is observed in isolation, as in our standard method. This approach usually resulted in a less precise but more robust measurement (i.e., one that passed our criteria for accuracy set forth below).

3.3. Reference frame and plotting conventions

The relative novelty of the site-specific carbon isotope fractionations being measured necessitates the definition of a reference frame for reporting and plotting variations in composition. Some, though not all, previous NMR-based studies of site-specific carbon isotopes have been able to draw on the capacity of that technique to observe absolute differences in ^{13}C content between sites. When such data are combined with known full molecular $\delta^{13}C$ values (for instance, through a conventional combustion-based analysis), it is possible to calculate the $\delta^{13}C$ of each site vs. some common scale (e.g., V-PDB) by mass balance. In other cases (Gilbert et al., 2013), NMR observes only the site-specific C isotope compositions of a subset of sites, meaning such mass balance constraints are not applicable and only differences in $\delta^{13}C$ between constrained sites can be reported.

We face a different problem. Gas source mass spectrometry exhibits an intrinsic analytical mass fractionation that must be corrected for by comparison with a known standard. Site-specific and clumped isotope standards potentially can be prepared by selective chemical degradation followed by conventional analysis of the 'pieces' (e.g., N_2O, Toyoda and Yoshida, 1999), or by driving a standard to thermodynamic equilibrium at known temperature and assuming theoretical values of that equilibrium state (e.g., CO_2, O_2, CH_4 and N_2O; Wang et al., 2004; Stolper et al., 2014b; Magyar et al., 2016; Piasecki et al., 2016b). Neither of these strategies has yet succeeded for propane; thus, we can only report variation in site-specific carbon isotope ratio as differences from a standard without knowing the absolute $^{13}C/^{12}C$ ratios of each carbon position.

The standard used for these measurements, Caltech Propane 1, or 'CITP1', was obtained from Air Liquide; it was presumably purified from a conventional natural gas of unknown origin. The $\delta^{13}C_{V\text{-}PDB}$ of the standard is $-33‰ \pm 0.55$, and the δD_{VSMOW} of the standard is $-197.7‰ \pm 1.4$. When we report the $\delta^{13}C$ of the terminal or central

position measured for some unknown sample, it is relative to a reference frame in which the $\delta^{13}C$ of the terminal and central position carbons of our standard, CITP1, are axiomatically set to equal zero. For clarity, all such values are reported as: $\delta^{13}C_{end}^{CITP1}$ or $\delta^{13}C_{center}^{CITP1}$. Identical values for these two parameters therefore mean only that a sample analyte has the same (unknown) $\delta^{13}C$ difference between terminal and central carbons as our CITP1 standard, and not that the difference is zero—for either sample or standard—in an absolute reference frame.

Reporting the results of theoretical calculations, we face none of these standardization problems and can simply give the calculated $\delta^{13}C$ value of each position, relative to any arbitrary reference frame such as V-PDB. In these cases, data are notated as $\delta^{13}C_{end}^{PDB}$ or $\delta^{13}C_{center}^{PDB}$.

Note that in the case of analytical data, the $\delta^{13}C$ of the terminal and center positions has been calculated by combination of two independent constraints. For example, the terminal position might be set equal to the measured value of a methyl fragment based on prior demonstration that the two are equivalent (Piasecki et al., 2016a). In contrast, the central position might be calculated based on the difference between the measured 1-carbon and 2-carbon fragment ions (see Piasecki et al., 2016b, for details). In all cases, we have propagated analytical errors for the constraint in question through the relevant mass-balance calculation.

4. RESULTS

All sample analyses, including supporting data such as independently measured bulk $\delta^{13}C$ values, are presented in Tables 1 and 2. Note that not all of the four possible measurements (molecular $\delta^{13}C$ measured as CO_2 by conventional IRMS; and $\delta^{13}C$ of 1-, 2-, or 3-carbon ions using the 253 Ultra) were made on all of the samples. Blank spaces in the data table indicate that those particular measurements were not performed on those samples.

Table 1 includes only data that pass two criteria for accuracy: (1) the molecular $\delta^{13}C$ value calculated from measurement of two or more fragment ions (or the three carbon species alone) must be consistent with the value determined by some other independent technique (generally online combustion GC-IRMS), with an accepted range of agreement of ±1‰. Note that this test is made after correcting for interlaboratory differences in standardization that result in self-consistent shifts of data for multiple samples run in two or more laboratories; such corrections are only significant for the Potiguar Basin suite. In the latter half of this study, as we moved to work on gases with lower propane abundance and greater proportions of the more troublesome contaminant gases (primarily CO_2), we also developed contamination indices based on the relative heights of peaks in the propane mass spectrum. (2) a measurement is considered valid only if its measured intensity ratios for 29/28, 43/42 and 44/43 are all within 20% of the value observed for a concurrently run standard, with no evidence for CO_2 or butane in the mass spectrum (Table 3). Data for samples that fail one or both of these metrics are presented in the appendix, but we do not attempt to interpret them. These problems do not arise from isobaric interferences which would be noted in scans of the mass spectrum near the analyzed peaks; rather, we suspect they arise from changes in the fragmentation behavior and associated instrumental mass fractionations when gases other than propane are present in the ion source. The quality score indicates whether all of these criteria are met with one being excellent and four being poor.

4.1. Range of natural samples

Four different sample groups were analyzed: hydrous pyrolysis experiments, gases from the Potiguar Basin in Brazil, which is a conventional natural gas reservoir, and shale gas samples from the Eagle Ford Shale and Antrim Shale. Despite the wide range of different formation mechanisms and protoliths, the samples all span a relatively small range of isotopic variation relative to the standard, with up to 15‰ variation in the terminal carbon and 10‰ in the central carbon. Replicate precision is listed in Table 1, but the standard error in the terminal measurement is ±0.5‰ for most measurements and 0.25‰ for the two carbon measurement due to the relative abundance of the different ions produced within the mass spectrometer. The molecular $\delta^{13}C$ values were calculated and compared to externally measured values, and generally found to be consistent with published data. In the case of the Potiguar Basin gases, the whole sample suite was offset by 0.5‰, which we believe to be due to a difference in standardization (discussed more in Section 5.3). The majority of the Potiguar suite and the experimental suite were measured in duplicate when possible, and replicates fall within one standard deviation of one another.

In general, there are some trends that are significant between the different samples. Further details of each sample suite will be discussed in Section 5. As expected from previous work, the $\delta^{13}C$ of both carbon sites increases with increasing thermal maturity (temperature in the case of experiments, vitrinite reflectance (Ro) for the Eagle Ford and Potiguar sample suites). For the natural samples the majority of the increase in $\delta^{13}C$ is seen at the terminal carbon, until a certain maturity threshold is reached, whereas in the experimental samples there is a larger change in the center position first. While the concavity of the natural versus experimental trends differ, the direction and order of magnitude of the change as a result of increasing maturation are similar, and we believe that the experiments provide useful insight into the natural samples.

Results from the hydrous pyrolysis experiments are shown in Fig. 3. Propane produced in the first stage of heating at 330 °C is characterized by a center position $\delta^{13}C$ value close to that of our reference gas. This is similar to that in relatively low $\delta^{13}C$ natural thermogenic propane (generally considered a sign of low to moderate maturity). The terminal position carbon, in contrast, is markedly low in $\delta^{13}C$, being 9‰ lower than our reference standard and similarly lower than the terminal carbon in any other natural propane analyzed in this study. Increasing temperature from 330 to 360 °C is associated with a modest (~1.5‰) increase in $\delta^{13}C$ of the terminal position but a larger (~4.5‰) increase in the center position. At 390 °C both

Table 1
This table contains all of the samples measured for the study. On the left half is the actual measured data. Blank spaces indicate that specific measurement was not performed on that sample. The calculations are done by combining the different fragment measurements as discussed in the text. For the Potiguar Basin suite, the letters after the names represent a replicate that was purified separately. Quality refers to a metric described in the text to judge the purity and reproducibility of the sample with 1 being the best and 4 the worst. Standard deviations are internal, as all samples were not replicated.

	Measurements											Calculations			
Sample	$\delta^{13}C_{end}$	st dev	st err	$\delta^{13}C_{ehtyl}$	st dev	st err	$\delta^{13}C_{full}$	stdev	st err	δD	st err	$\delta^{13}C_{end}$	$\delta^{13}C_{center}$	$\delta^{13}C_{full}$	Quality
Diffusion experiments															
Dif_1	−3.21	1.99	0.35	−3.50	0.59	0.11						−3.21	−3.80	−3.41	2
Dif_3	−3.32	1.90	0.34	−3.53	0.73	0.13						−3.32	−3.74	−3.46	2
Res_1	2.34	2.82	0.58	1.60	0.40	0.07						2.34	0.86	1.85	2
Res_3	1.52	1.85	0.34	1.27	0.59	0.10						1.52	1.01	1.35	2
Hydrous pyrolysis experiments															
330-72-1-1	−9.01	1.84	0.33	−3.59	1.23	0.22						−9.01	1.83	−5.39	2
360-72-1-1	−6.94	2.75	0.49	−0.84	0.85	0.15						−6.94	5.26	−2.87	2
360-72-2A	−8.57	1.96	0.35	−0.25	0.32	0.06						−8.57	8.06	−3.03	2
390-72-1-2				2.78	0.29	0.05	0.40	0.16	0.03	64.67	2.05	−4.36	9.91	0.40	3
Potiguar basin suite															
011359-01a	6.82	1.65	0.24	4.88	0.85	0.13						6.82	2.94	5.53	2
011359-01b	4.67	1.62	0.26	5.67	0.51	0.08						4.67	6.66	5.33	2
011359-02	1.66	1.69	0.69	0.46	0.67	0.12						1.66	−0.74	0.86	2
011359-03a	4.84	2.41	0.38	3.72	0.39	0.07						4.84	2.59	4.09	2
011359-03 b	3.19	1.76	0.31	1.41	0.84	0.12						3.19	−0.37	2.00	2
011359-03c	4.58	1.11	0.24	0.41	1.42	0.25						4.58	−3.77	1.80	2
011359-04a	4.55	1.92	0.34	4.29	0.51	0.09						4.65	3.94	4.41	2
011359-04b	4.56	1.50	0.22	5.53	1.17	0.19						4.56	6.51	5.21	2
011359-04c	6.28	1.89	0.33	4.73	0.63	0.11						6.24	3.23	5.23	2
011359-07a	0.76	2.96	0.52	0.05	0.38	0.29						0.76	−0.67	0.28	2
011359-07b	0.17	2.68	0.42	−0.22	0.61	0.11						0.17	−0.60	−0.09	2
011359-09	3.53	0.82	0.17	1.64	1.17	0.21						3.53	−0.24	2.27	2
Eagle ford suite															
Emma Tartt 25	−23.70	5.73	1.17	3.26	0.33	0.06	3.54	0.27	0.05	−66.58	2.01	4.09	2.44	3.54	4
Emma Tartt 22H	−47.72	2.02	0.36	2.87	0.41	0.07	3.25	0.78	0.14	−68.36	1.75	4.00	1.75	3.25	4
Irvin Mineral South 1H	−24.80	5.75	1.02	3.75	0.31	0.06	4.32	0.23	0.04			5.47	2.03	4.32	4
Antrim suite															
C2-31-1-1				−1.12	0.22	0.04	−1.34	0.12	0.02	−8.01	1.64	−1.79	−0.46	−1.34	3
Standard							−33.23	0.55		−179.7	1.4				

Table 2
This table contains measurements of $\delta^{13}C$ done by external labs on the different constituents of the natural gas samples including percentage of different alkane components.

	External data									
Sample	$\delta^{13}C$ CH_4	$\delta^{13}C$ C_2H_6	$\delta^{13}C$ C_3H_8	$\delta^{13}C$ nC_4H_{10}	$\delta^{13}C$ iC_4H_{10}	% CH_4	% C_2H_6	% C_3H_8	% nC_4H_{10}	% iC_4H_{10}
Hydrous pyrolysis experiments										
330-72-1-1	−43.55	−38.15	−35.55	−33.66		49.30	27.54	14.22	4.49	1.62
360-72-1-1	−44.62	−34.45	−32.81	−31.44	−31.48	55.07	25.32	12.56	3.59	1.37
360-72-2A	−44.62	−34.45	−32.81	−31.44	−31.48	55.07	25.32	12.56	3.59	1.37
390-72-1-2	−38.72	−29.89	−29.77	−28.92	−29.39	70.08	16.83	8.21	2.12	1.27
Potiguar basin suite										
011359-1	−40.79	−31.21	−29.29	−28.49	−27.94					
011359-01a	−40.79	−31.21	−29.29	−28.49	−27.94					
011359-02b	−48.25	−38.01	−34.81	−33.75	−34.64					
011359-3	−47	−34.84	−32.26	−31.75	−33.52					
011359-3 b	−47	−34.84	−32.26	−31.75	−33.52					
011359-03a	−47	−34.84	−32.26	−31.75	−33.52					
011359-4	−45.02	−32.61	−29.84	−29.4	−31.28					
011359-4	−45.02	−32.61	−29.84	−29.4	−31.28					
011359-04a	−45.02	−32.61	−29.84	−29.4	−31.28					
011359-07a	−47.14	−36.79	−34.27	−33.51	−34.53					
011359-7m	−47.14	−36.79	−34.27	−33.51	−34.53					
011359-9	−44.19	−32.87	−30.68	−30.87	−31.65					
Eagle ford suite										
Emma Tartt 25	−45.55	−33.60	−29.30	−28.70	−31.60	77.86	11.88	4.94	0.98	0.45
Emma Tartt 22H	−46.08	−33.50	−28.80	−29.10	−31.70	67.41	15.78	9.63	2.06	0.95
Irvin Mineral South 1H	−47.40	−32.20	−29.32	−30.03	−31.20	77.80	12.62	5.32	1.28	0.58
Antrim suite										
C2-31-1-1	−53.3					69.75	6.62	1.97	0.05	0.10

Table 3
This table contains the ratios used to confirm that pure propane is being measured.

	Contamination indices				
Sample	29/28	43/42	45/44	44/43	58/57
Hydrous pyrolysis experiments					
330-72-1-1	Out of gas	3.57	0.03	0.96	
360-72-1-1	1.60	3.54	0.03	1.04	
360-72-2A	1.63	4.34	0.03	1.06	0.05
390-72-1-2	1.63	4.35	0.03	1.14	
Eagle ford suite					
Emma Tartt 25	1.54	4.80	0.03	1.05	0.01
Emma Tartt 22H	1.53	4.72	0.03	0.95	0.03
Irvin Mineral South 1H	1.55	4.82	0.03	1.11	
Antrim suite					
C2-31-1-1	1.59	5.37	0.03	1.07	
Standard	1.62	5.21	0.03	1.24	

sites increase in $\delta^{13}C$ further. We discuss the implications of these findings in Section 5.3, after reviewing our data for natural gases.

5. DISCUSSION OF EXPERIMENTAL AND NATURAL SAMPLES

5.1. Expected patterns of site-specific carbon isotope variation in thermogenic propane

The site-specific carbon isotope composition of propane from natural environments could reflect a variety of processes: (a) equilibrium thermodynamic partitioning (which promotes concentration of ^{13}C in the central position, according to Webb and Miller (2014) and Piasecki et al. (2016a); (b) biological consumption or production (Hinrichs et al., 2006); (c) photochemical oxidation in the atmosphere (Takenaka et al., 1995); or (d) thermally activated destruction (both mixing and diffusion appear not to produce site-specific fractionations within propane (Piasecki et al., 2016a,b). However, kinetic isotope effects associated with kerogen and alkyl 'cracking' reactions during thermogenic gas production are likely to dominate the carbon isotope structures of propane in most propane-rich natural gases, and are the most relevant to the samples explored in this study. Therefore, we focus our interpretation on kinetic isotope effects altering preexisting or inherited structures, while acknowledging that other mechanisms, like aerobic or anaerobic oxidation by microbial activity, could dominate in other environments. The possible site-specific carbon isotope variations associated with thermogenic propane production were first predicted implicitly by the model of Chung et al. (1988), and modeled using first-principles theory and pyrolysis experiments by Tang et al. (2000). Both Gilbert et al. (2016) and Piasecki et al. (2016b) present discussions and extrapolated predictions based on these earlier papers. Fig. 1 summarizes position-specific carbon isotope variations in thermogenic propane as predicted by Piasecki et al. (2016b).

The simplest case presented in Fig. 1, based on the model of Chung et al. (1988), is kinetically controlled cracking of an *n*-alkane precursor molecule, with a kinetic isotope effect (KIE) only acting on the carbon in propane that was adjacent to the cleaved bond. This will result in one terminal end of propane being lower in $\delta^{13}C$ than the precursor by an amount equal to the KIE of the cracking reaction, whereas the central position and other terminal position are inherited without fractionation from the precursor (Chung et al., 1988). Piasecki et al. (2016b) also consider a variant of the model proposed by Chung et al. (1988), where the precursor is an isoprenoid and the carbon adjacent to the cleaved bond is in the central position, such that both terminal positions of propane are inherited from the precursor without fractionation and the central position is lower in $\delta^{13}C$ than the precursor by an amount equal to the KIE. The third model considered by Piasecki et al. (2016b) is the Tang et al. (2000) treatment, which predicts the effects of cracking an *n*-alkane (as in Chung et al., 1988), but with KIEs that are predicted by first-principles theory and effect all three of the carbon positions in product propane. An important caveat to all of these models is the assumption that the precursor is homogeneous in carbon isotope composition—almost certainly an over simplification. Gilbert et al. (2013) measured the differences in $\delta^{13}C$ between the three terminal carbon atom positions (CH_3, CH_{2a} and CH_{2b} groups) in several *n*-alkanes using NMR, revealing 10+‰ site-specific variations among the carbons that could go into propane formed by cracking such compounds. In Fig. 1, the site-specific compositions of these three terminal positions are plotted for the averages of three major patterns of isotopic structure identified by Gilbert et al. (2013). These are the compositions expected for propane if it formed from these compounds without any isotopic fractionation. Thus, the set of all predicted compositions could be deduced by overlaying the three fractionation vectors in Fig. 1 on each of the three possible starting compositions. Note, however, that Gilbert et al. (2013) examined samples of commercially produced *n*-alkanes with an unknown relationship to natural organic matter. Thus, the variations we summarize from that study should be considered illustrative of possible ranges in composition, without being relatable to any specific natural propane precursor.

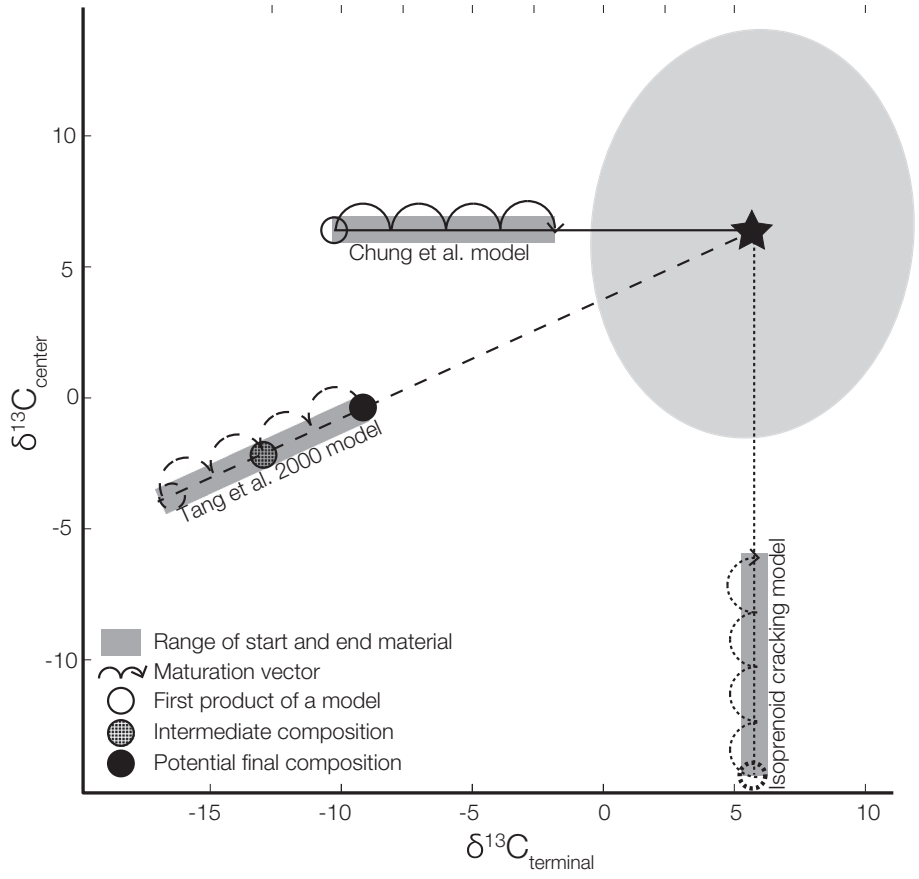

Fig. 1. Expected site-specific fractionations from idealized cracking of propane. Following the Chung diagram assumption, not data, maturation should move left to right, while source will affect both terminal and center positions equally. Modified from (Piasecki et al., 2016a,b).

5.2. Hydrous pyrolysis experiments

We first explore the catagenetic models outlined above by measurements of propane produced experimentally by hydrous pyrolysis of organic-rich shale. These experiments provide at least a first look at the experimental basis for using site-specific carbon isotope composition of propane as a proxy for thermal maturity in natural gas basins. Given that all hydrous pyrolysis experiments were conducted for the same length of time, and were performed in sequence from the same starting material, higher temperatures should represent higher thermal maturity.

We infer that the gas generated in the 330 °C experiment was created dominantly from degradation of kerogen (i.e., because the original sample was thermally immature and the residual non-gaseous organics after heating were predominantly kerogen; Fig. 2). For the purposes of this paper, we define kerogen as the insoluble, immobile organic component of source rocks, bitumen as the solvent-extractable but immobile organic component, and oil as the free liquid-phase (mobile) organic component. After further heating at 360 °C, residual kerogen and bitumen have decreased dramatically and the dominant non-gaseous organic compound is oil. Propane produced during this heating step may be a mixture of products from decomposition of all three of these components, but it seems likely that bitumen decomposition is a greater contributor here than in the lower or higher temperature steps due to the measured propane composition relative to that of the other temperature steps. Further heating at 390 °C creates continued decreases in kerogen and bitumen, but also even greater degradation of earlier-generated oil (the majority of the hydrocarbons in this sample were natural gas). We

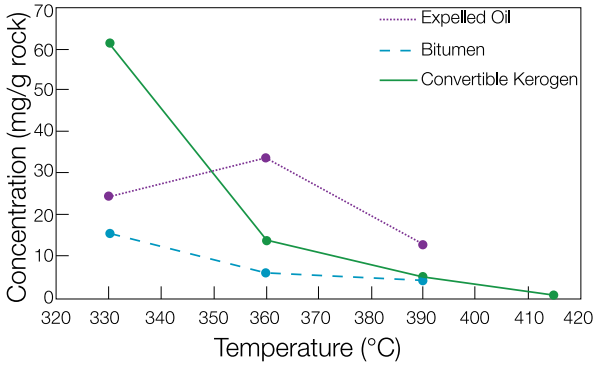

Fig. 2. Different components as a function of temperature within the hydrous pyrolysis experiments.

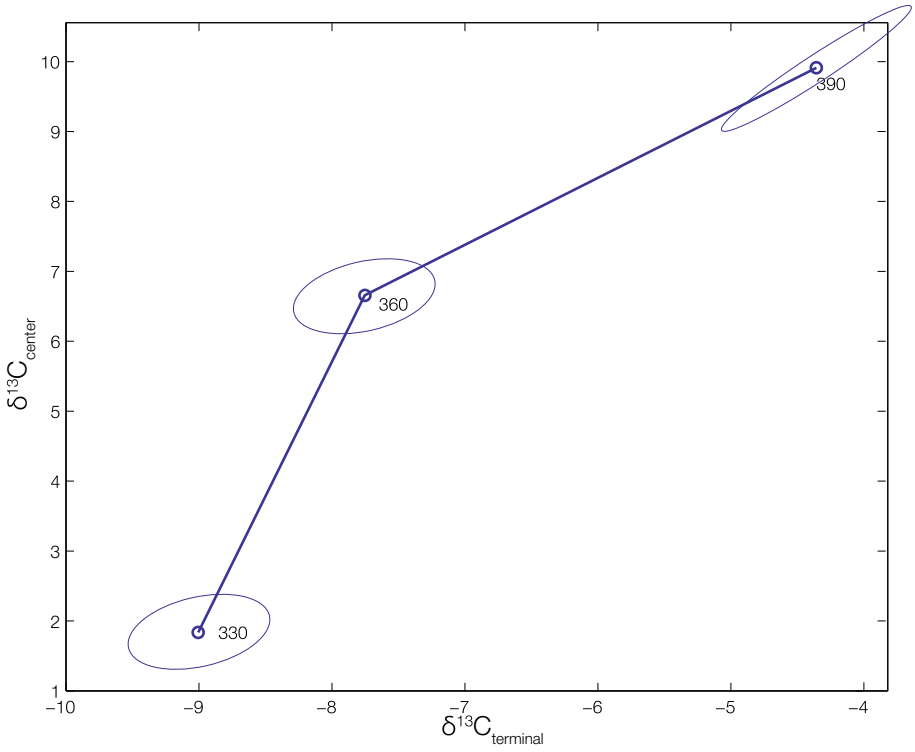

Fig. 3. Isotopic results of experiments conducted on natural samples. The temperature (in °C) of each experiment is shown beside the data point. All experiment times are 72 h, and results are relative to the Caltech standard (CITP1). Error ellipse is for internal standard deviation except for the 360 °C experiment where it is external due to replication.

conclude that propane in this gas fraction likely also has contributions from all three source substrates, but contains a relatively high fraction of propane produced from oil. The highest temperature experiment conducted at 415 °C leaked and was fractionated, there are therefore no data for that experiment.

For experiments reaching 330 °C and 360 °C, the whole-molecule $\delta^{13}C$ values of propane calculated from measurements of C_1 and C_2 fragment ions matched the $\delta^{13}C$ values from GC-IRMS within error. However, the 390 °C experiment resulted in an implausibly low $\delta^{13}C$ value for the methyl fragment ion, a common feature of samples that are contaminated. It is unknown why only this one sample was apparently contaminated, and we speculate that it was related to minor volatile components that entered the gas phase during higher reaction temperature. Regardless, for this sample we also measured the C_3 molecular ion. This latter measurement agrees with the GC-IRMS value, and combining it with our measurement of the C_2 fragment constrains the difference in $\delta^{13}C$ between center and terminal positions.

5.3. Natural propane from the Potiguar Basin

In this section, we describe measurements of the site-specific carbon isotope composition of propane from the Potiguar Basin described above in the background section. Assuming that the full molecular $\delta^{13}C$ of propane is a proxy for thermal maturity (Chung and Sackett, 1979; Chung et al., 1988; Tang et al., 2000; Ni et al., 2011), the most noticeable feature of the Potiguar data is that it exhibits the opposite pattern from Woodford Shale hydrous pyrolysis experiments. That is, starting at the lightest $\delta^{13}C$ (lowest maturity), first the $\delta^{13}C$ of the terminal position increases, then at higher maturity the center position rises markedly with modest additional increase in the terminal position. Potiguar Basin propanes exhibit site-specific $\delta^{13}C$ values similar to or enriched in ^{13}C relative to our reference standard, for both positions (Fig. 4). While we know little about this intralab working standard, it is likely that it comes from a relatively propane-rich, and thus low-maturity, thermogenic natural gas.

The Potiguar data could potentially be reconciled with the Woodford Shale pyrolysis experiments in two different ways. First, the Potiguar samples may be of lower equivalent maturity than the hydrous pyrolysis experiments, such that the latter half of Fig. 4 (rapid rise in central $\delta^{13}C$) corresponds to the first half of Fig. 3. In this case, the two sets of data are manifesting the same basic behavior, but start and end at different thermal maturities. Second, the dominantly Type-1 source kerogens of the Potiguar Basin could be rich in *n*-alkyl carbon skeletons relative to the Type-II Woodford Shale, leading to a more dominant role of cracking terminal *n*-propyl groups and consequent isotope fractionation mainly at terminal positions. Experiments that start with a more simple long chain n-alkane starting material of known isotopic structure could elucidate this theory, and experimentally confirm the results of Tang et al. (2005)

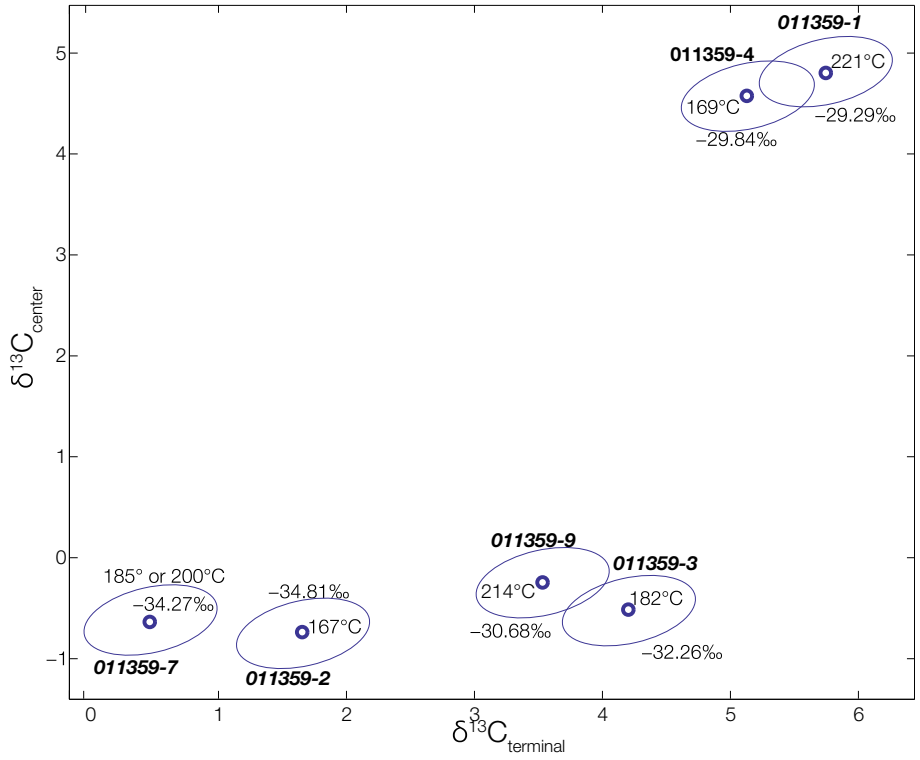

Fig. 4. Internal isotope distribution on a suite of wet gases from the Potiguar Basin, and results are relative to the Caltech standard (CITP1). The number label in per mil is the externally measured carbon isotope value. The label in bold italic is sample name. The final label is the temperature as measured by Stolper et al. (2014b) for the methane formation temperature. Internal standard deviation is shown by error ellipse when data point is not replicated. Distribution of data shows that there is an effect both on the center and terminal position as maturity changes.

on how distance from cleaved bonds affects propane generation after a series of these kinetic steps.

Regardless of how we reconcile the Potiguar data with existing hydrous pyrolysis experiments, it remains to explain why terminal and central carbon positions rise at different and changing rates as we transition from low bulk $\delta^{13}C$ and low inferred thermal maturities to high bulk $\delta^{13}C$ and high inferred thermal maturities. One plausible interpretation of the Potiguar Basin data is that they capture the transition from propane production from kerogen substrates to propane production from bitumen or oil substrates. This interpretation is at least generally consistent with the previous interpretation of the clumped isotope thermometry of Potiguar Basin methanes, which suggested mixing between low $\delta^{13}C$, wet gases of moderate maturity and higher $\delta^{13}C$, higher maturity gases, creating higher gas to oil ratios (Stolper et al., 2014b). If this explanation of our data holds true, site-specific carbon isotope compositions of natural propanes could provide a significant new proxy for the production of gas from mobile hydrocarbons (as opposed to kerogen).

A complication of our dataset is that the evolution of apparent maturity of the propane does not correspond with the methane formation temperature measured in a previous study on the same samples (Stolper et al., 2014b). This could reflect the possibility that the shift in the organic precursor molecule for propane occurred over a relatively narrow range of temperature and has little connection to the wider range of temperatures of methanogenesis that controls the correlation between methane formation temperature and methane $\delta^{13}C$. The temperature is defined in Stolper et al. (2014b) and is measured in the coexisting methane for the exact same samples, and the change in precursor is suggested as the mechanism to change the central carbon position within the propane following the hydrous pyrolysis experiments. For example, the methane formation temperatures could reflect a contribution from a high maturity, dry gas that does not contribute propane to the bulk fluid. In such a scenario, the methane clumped isotope temperature of the bulk fluid would continue to increase but will be decoupled from the propane systematics observed here.

5.4. Natural propane from the Eagle Ford Shale

We also examined samples of natural propane from the Eagle Ford Formation in Texas. The Eagle Ford gases examined in this study are relatively rich in CO_2, and despite our efforts to purify them, all but three of the samples failed one or both of our quality control criteria. Herein we focus solely on data for the three samples that did pass these criteria—Emma Tartt 22H and 25, and Irvin Mineral South 1H (Fig. 5). Unfortunately, these three gases encompass only a narrow range of relatively low maturity in this suite.

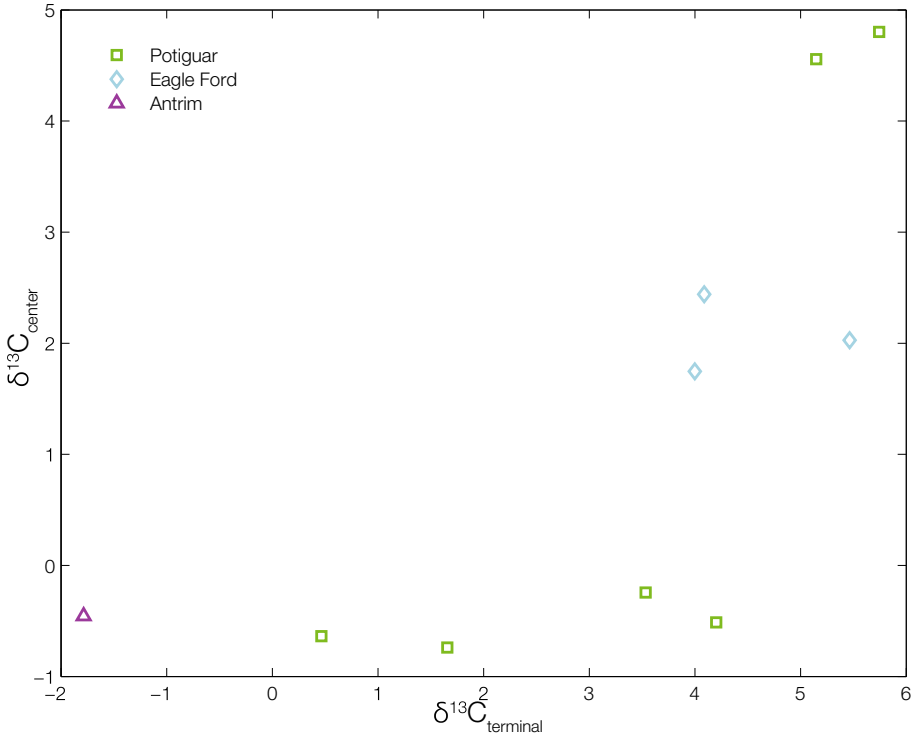

Fig. 5. Data for all of the samples measured, excluding lab diffusion experiments. This includes the Eagle Ford and Antrim samples, which were previously not shown in figures.

The results for these three samples define a closely grouped set of compositions that lie within the range spanned by the Potiguar Basin suite (Fig. 5). If we attempt to interpret their average composition in a way that is consistent with both our Woodford Shale hydrous pyrolysis experiments and interpretations of the Potiguar Basin gases, we conclude that these Eagle Ford Shale gases contain the products of a mixture of propane produced early in the catagenetic process through breakdown of kerogen combined with products of later breakdown of bitumen and/or oil components (i.e., because these gases lie in the middle of the inferred maturity trend for the Potiguar samples, and are intermediate in center position $\delta^{13}C$ when compared with the known maturity sequence of the experiments). This is consistent with observations on saturate and aromatic fractions of the coexisting oils sampled from these wells that display signs of early oil cracking. The plausibility of this preliminary conclusion is also supported by the fact that these gases come from an unconventional shale deposit, which is believed to integrate products across a range of maturities.

5.5. A natural propane from the Antrim Shale

The Antrim Shale is the final sample and is unique relative to the other suites in the study due to the potential of microbial oxidation in the basin. However, we found Antrim Shale gases to be highly problematic as targets for our measurement because most are poor in propane and many are rich in CO_2. As a result, only one sample passed our criteria for sample purity. We do not have independent measurements of molecular $\delta^{13}C$ for propane, but prior work on this sample suite indicates the range of plausible values, which is consistent with our result for the one sample analyzed in this study based on analyses of the C_2 and C_3 fragment ions. The sample is a relatively wet gas (relative to other members of the Antrim suite), and has a site-specific carbon isotope composition for propane ($\delta^{13}C^{end}_{CITP1} = -1.8‰$ and $\delta^{13}C^{center}_{CITP1} = -0.4‰$) that resembles the lowest maturity end of the range for the Potiguar Basin suite (Fig. 5). This is consistent with prior claims that the thermogenic component of Antrim Shale gases has low thermal maturity, and is consistent with the recent finding by (Stolper et al., 2015) that the component of thermogenic methane in these gases formed at relatively low temperature (~115 °C, or early in the primary kerogen cracking window). It is likely that this result provides little insight into the isotopic effects of biological propane oxidation, as it was measured on a propane-rich sample having a relatively low propane $\delta^{13}C$ value ($\delta^{13}C_{PDB} = -34‰$) that is uncharacteristic of residual biodegraded propane.

5.6. Insights into the mechanisms of propane formation

Perhaps the most noteworthy feature of our results is that both experiments and measurements of natural samples suggest that the isotopic composition of propane evolves with increasing maturity in a distinctive way, with a progressive rise in molecular $\delta^{13}C$ (as expected) but including a sharp step up in the $\delta^{13}C$ of the center carbon, over what seems to be a narrow part of the maturity range defined by the temperature of experiment or coexisting

methane sample. It seems likely that further work on this problem will reveal a variety of influences on the site-specific isotopic structure of propane, such as source rocks, rates and conditions of reaction, chemistry of coexisting fluids, and perhaps other factors. However, the trends in Figs. 3–5 suggest the following organizing hypothesis.

Two features of our findings—the low $\delta^{13}C$ of the terminal site in our 330 °C experiments, and the 'flat' trajectory of the vector defined by the lowest $\delta^{13}C$ natural samples in Fig. 5—suggest that the earliest stages of catagenetic propane production include 'cracking' reactions that impose a strong kinetic isotopic fractionation on the C—C bond adjacent to what will become one of the terminal carbon sites, and that the rising temperatures and advancing reaction progress associated with increases in maturity diminish this effect (i.e., as in Chung et al. (1988) and Tang et al. (2000)). It is important to note that the later kinetic studies of Tang et al. (2000) include a predicted effect on the center carbon as well as the terminal carbon of the generated propane. This predicted increase of slope of is not observed. Therefore, this distal isotope effect is not as prominent as the modeling suggests, or the degradation of created propane to smaller species somehow masks this predicted result.

Two other observations—the sharp rise in central position $\delta^{13}C$ in both the 360 °C experiments and the natural samples in the upper half of the overall $\delta^{13}C$ range—suggest that at some moderate to high level of maturity propane synthesis undergoes a significant change in the molecular and/or isotopic structure of the substrates that make up its dominant sources. This could include a reduction in the importance of isoprenoid compounds as a fraction of those substrates, and/or a shift from substrates having isotopic structures resembling short-chain alkanes to those having isotopic structures more like long-chain alkanes (Gilbert et al., 2013).

It is noteworthy that the rise in center-position $\delta^{13}C$ in experiments is associated with a transition from kerogen-dominated to a bitumen- and oil-dominated residue. This raises the possibility that the shift in substrate molecular and/or isotopic structure we hypothesize above is actually a mark of the transition from kerogen cracking to bitumen or oil cracking due to the depletion of kerogen within the experiment. If so, this could result in a significant new geochemical tool for exploring the sources of petroleum and/or fingerprinting the geological origins of fugitive natural gas emissions. A variety of geochemical proxies have been suggested to constrain the relative contributions of kerogen vs. oil to natural gas production. However, none are specific to bitumen (which seems like the most likely control of the 360 °C experiment), and none suggest the potential we see here for a geochemical proxy that is based on a single compound, quite 'sharp' (i.e., occurs over a narrow maturity interval), and high in amplitude. Testing and refining this hypothesis will have to include more new data constraining the isotopic structures of petroleum precursors and fractionations associated with catagenesis.

One further complication not discussed to this point is the variation in the bulk $\delta^{13}C$ of source kerogens; i.e., propane produced from two source facies having substrates with similar isotopic structures, and reaching a similar maturity, would still differ in molecular $\delta^{13}C$ if those two sources differ in their initial bulk $\delta^{13}C$. Given the potential importance of the differences in substrate molecular and isotopic structure in dictating the carbon isotope structure of derived propane, we should expect that differences in $\delta^{13}C$ between two different sources (e.g., lacustrine vs. marine shales vs. coals) might also be associated with differences in site-specific carbon isotope structures of kerogens or other components of those sources. Substantially more experimental work on the products of cracking experiments performed on diverse source materials will be required to better understand this issue.

6. CONCLUSIONS

Previous studies provide a framework for understanding the evolution of carbon isotopes in natural gas systems (Chung and Sackett, 1979; Chung et al., 1988; Schimmelmann et al., 1999; Tang et al., 2000, 2005; Lorant et al., 2001; Hill et al., 2003; Zou et al., 2007; Ma et al., 2008; Ni et al., 2011). Herein, we extend this framework via a new measurement of the isotopic structure of a natural hydrocarbon. The results of our measurements, specifically Figs. 3–5, show that thermogenic propane, both in experiments and nature, exhibits systematic variations in carbon isotope structure with increasing molecular $\delta^{13}C$ and thermal maturity. These variations are not easily explained by any one previous model of the carbon isotope geochemistry of natural gas components (or other models we suggest here), but point toward a richer understanding that combines several factors: fundamental kinetic isotope effects associated with 'cracking' reactions; diversity in the molecular structures of substrates from which propane is formed; and diversity in the isotopic structures of these precursor compounds. It is perhaps unsurprising that all of these factors should be important to the stable isotope geochemistry of petroleum and natural gas compounds. However, the possibility of concretely advancing our understanding of these issues through experiment and studies of the intramolecular isotopic structures of natural samples is new, and will presumably grow with further application of emerging analytical techniques of high-resolution mass spectrometry (this study), NMR (Gilbert et al., 2013) and perhaps other methods (Gilbert et al., 2015).

The experiments involving pyrolysis of Woodford Shale offer the most constrained system examined in this study, and suggest that the shifts from kerogen, to bitumen, and finally to oil as the dominant non-gaseous hydrocarbons corresponds to a large (~5‰) increase in the C isotope composition of the central carbon position of propane, combined with the general increase in $\delta^{13}C$ for the terminal position carbon.

The natural gases from the Potiguar Basin, Antrim Shale and Eagle Ford Shale suites could be interpreted to reflect a similar shift from kerogen to bitumen and/or oil cracking with increasing maturity. In particular, it would be reasonable to speculate that the set of five gases that all share a common, low $\delta^{13}C$ value for the center carbon position (one from Antrim and four from Potiguar Basin) were generated by primary cracking of kerogen, with

increasing extents of reaction driving product propane to the right in Fig. 5 (increasing $\delta^{13}C$ of the terminal position) due to kinetic isotope effects. We suggest that the heavier $\delta^{13}C$ values for the center carbon position seen in the remaining five samples (the highest $\delta^{13}C$ Potiguar samples and the Eagle Ford samples) reflect a shift in the substrate from which propane is generated at high maturities, perhaps including increased contributions from decomposition of bitumen and/or oil, i.e., that this 'jog' in the overall trend for natural samples marks the point in the maturity scale where propane from these non-kerogenous precursors becomes a significant fraction of all propane. This could be taken as evidence that the Eagle Ford propane is a mixture of the products of kerogen and oil cracking, or simply a portion of the way along that evolutionary pathway.

Finally, it is also expected that variations in the isotopic structure of propane could be influenced by thermal degradation of propane—a type of 'secondary cracking' reaction. Propane readily degrades to form smaller hydrocarbons (mostly methane) upon heating, particularly in the presence of catalysts. Simple disproportionation of propane, involving rupture of the C—C bond between terminal and center positions, would presumably enrich the $\delta^{13}C$ of both sites in the residue, though we cannot easily predict how strong these effects could be, nor if they would be equal. If, instead, propane forms a complex with an active or catalytic surface before it 'cracks,' we might expect to see different isotope effects, potentially where residual propane becomes lower in $\delta^{13}C$, not higher, due to the tendency of heavy isotopes to form complexes with this active surface. Further work is needed to understand the complex processes and chemical reactions that occur in natural gas systems, which requires experimental data or observations of natural samples where propane 'cracking' is known to have occurred.

ACKNOWLEDGEMENTS

This work was funded by an NSF-EAR instruments and facilities grant EAR-0949336. Additional funding was supplied by Exxon Mobil and Petrobras. The reviewers provided helpful comments especially about the structure of the manuscript. Any use of trade, firm, or product names is for descriptive purposes only and does not imply endorsement by the U.S. Government.

APPENDIX A. SUPPLEMENTARY MATERIAL

Supplementary data associated with this article can be found, in the online version, at https://doi.org/10.1016/j.gca.2017.09.042.

REFERENCES

Abelson P. H. and Hoering T. C. (1961) Carbon isotope fractionation in the formation of amino acids by photosynthetic organisms. *Proc. Natl. Acad. Sci. U.S.A.* **47**, 623.

Bertani R. T., Costa I. G. and Matos R. M. D. (1990) Evolução tectono-sedimentar, estilo estrutural e habitat do petróleo na Bacia Potiguar. In *Origem e Evolução de Bacias Sedimentares* (eds. G. P. Raja Gabaglia and E. J. Milani), pp. 291–310.

Betson T. R., Augusti A. and Schleucher J. (2006) Quantification of deuterium isotopomers of tree-ring cellulose using nuclear magnetic resonance. *Anal. Chem.* **78**, 8406–8411.

Caer V., Trierweiler M., Martin G. J. and Martin M. L. (1991) Determination of site-specific carbon isotope ratios at natural abundance by carbon-13 nuclear magnetic resonance spectroscopy. *Anal. Chem.* **63**, 2306–2313.

Chung H. M. and Sackett W. M. (1979) Use of stable carbon isotope compositions of pyrolytically derived methane as maturity indices for carbonaceous materials. *Geochim. Cosmochim. Acta* **43**, 1979–1988.

Chung H. M., Gormly J. R. and Squires R. M. (1988) Origin of gaseous hydrocarbons in subsurface environments: theoretical considerations of carbon isotope distribution. *Chem. Geol.* **71**, 97–104.

Clog M., Eiler J., Guzzo J. V. P., Moraes E. T. and Souza I. V. A. (2013) Doubly 13C-substituted ethane. *Mineral. Mag.* **77**, 805–933.

DeNiro M. J. and Epstein S. (1977) Mechanism of carbon isotope fractionation associated with lipid synthesis. *Science* **197**, 261–263.

Eiler J., Clog M., Magyar P. and Piasecki A. (2012) A high-resolution gas-source isotope ratio mass spectrometer. *Int. J. Mass Spectrom.*.

Eiler J., Blake G. A., Dallas B., Kitchen N., Lloyd M. K. and Sessions A. L. (2014) Isotopic anatomies of organic compounds. In *Goldschmidt Conference*.

Gao L., He P., Jin Y., Zhang Y., Wang X., Zhang S. and Tang Y. (2016) Determination of position-specific carbon isotope ratios in propane from hydrocarbon gas mixtures. *Chem. Geol.* **435**, 1–9.

Gilbert A., Silvestre V., Robins R. J., Remaud G. S. and Tcherkez G. (2012) Biochemical and physiological determinants of intramolecular isotope patterns in sucrose from C3, C4 and CAM plants accessed by isotopic 13C NMR spectrometry: a viewpoint. *Nat. Prod. Rep.* **29**, 476–486.

Gilbert A., Yamada K. and Yoshida N. (2013) Exploration of intramolecular 13C isotope distribution in long chain n-alkanes (C11–C31) using isotopic 13C NMR. *Organ. Geochem.* **62**, 56–61. https://doi.org/10.1016/j.orggeochem.2013.07.004.

Gilbert A., Suda K., Yamada K., Ueno Y. and Yoshida N. (2015) Position-Specific 13C Isotope Composition of Non-Methane Hydrocarbons. *Goldschmidt Abstracts 1040*.

Gilbert A., Yamada K., Suda K., Ueno Y. and Yoshida N. (2016) Measurement of position-specific 13C isotopic composition of propane at the nanomole level. *Geochim. Cosmochim. Acta* **177**, 205–216.

Guy R. D., Fogel M. L. and Berry J. A. (1993) Photosynthetic fractionation of the stable isotopes of oxygen and carbon. *Plant Physiol.* **101**, 37–47.

Hammes U., Eastwood R., McDaid G., Vankov E., Gherabati S. A., Smye K., Shultz J., Potter E., Ikonnikova S. and Tinker S. (2016) Regional assessment of the Eagle Ford Group of South Texas, USA: Insights from lithology, pore volume, water saturation, organic richness, and productivity correlations. *Int.-a J. Subsurface Character.* **4**, SC125–SC150.

Hill R. J., Tang Y. and Kaplan I. R. (2003) Insights into oil cracking based on laboratory experiments. *Org. Geochem.* **34**, 1651–1672.

Hinrichs K. U., Hayes J. M., Bach W., Spivack A. J., Hmelo L. R., Holm N. G., Johnson C. G. and Sylva S. P. (2006) Biological formation of ethane and propane in the deep marine subsurface. *Proc. Natl. Acad. Sci.* **103**, 14684–14689.

Lewan M. D. (1983) Effects of thermal maturation on stable organic carbon isotopes as determined by hydrous pyrolysis of Woodford Shale. *Geochim. Cosmochim. Acta* **47**, 1471–1479.

Lewan M. D. (1985) Evaluation of petroleum generation by hydrous pyrolysis experimentation. *Phil. Trans. R. Soc. A* **315**, 123–134.

Lewan M. D. (1993) Laboratory simulation of petroleum formation: hydrous pyrolysis. In *Organic Geochemistry Principles and Applications* (eds. M. H. Engel and S. A. Macko). Plenum, New York, pp. 123–134.

Lewan M. D. (1997) Experiments on the role of water in petroleum formation. *Geochim. Cosmochim. Acta* **61**, 3691–3723.

Lorant F., Behar F., Goddard W. A. and Tang Y. (2001) Ab initio investigation of ethane dissociation using generalized transition state theory. *J. Phys. Chem.* **105**, 7896–7904. Available at: <http://pubs.acs.org/doi/abs/10.1021/jp004094a>.

Ma Q., Wu S. and Tang Y. (2008) Formation and abundance of doubly-substituted methane isotopologues. *Geochim. Cosmochim. Acta* **72**, 5446–5456. https://doi.org/10.1016/j.gca.2008.08.014.

Macko S. A., Fogel M. L., Hare P. E. and Hoering T. C. (1987) Isotopic fractionation of nitrogen and carbon in the synthesis of amino acids by microorganisms. *Chem. Geol.: Isotope Geosci. Sect.* **65**, 79–92.

Magyar P. M., Orphan V. J. and Eiler J. (2016) Measurement of rare isotopologues of nitrous oxide by high-resolution multi-collector mass spectrometry. *Rapid Commun. Mass Spectrom.* **30**, 1923–1940.

Martini A. M., Walter L. M., Ku T. C. W., Budai J. M., McIntosh J. C. and Schoell M. (2003) Microbial production and modification of gases in sedimentary basins: a geochemical case study from a Devonian shale gas play, Michigan basin. *Bulletin* **87**, 1355–1375.

Mello M. R., Gaglianone P. C., Brassell S. C. and Maxwell J. R. (1988) Geochemical and biological marker assessment of depositional environments using Brazilian offshore oils. *Mar. Pet. Geol.* **5**, 205–223.

Mello M. R., Koutsoukos E., Neto E., and Telles, Jr., A. (1993). Geochemical and Micropaleontological Characterization of Lacustrine and Marine Hypersaline Environments from Brazilian Sedimentary Basins: Chapter 3.

Monson K. D. and Hayes J. M. (1980) Biosynthetic control of the natural abundance of carbon 13 at specific positions within fatty acids in Escherichia coli. Evidence regarding the coupling of fatty acid and phospholipid synthesis. *J. Biol. Chem.* **255**, 11435–11441.

Monson K. D. and Hayes J. M. (1982) Carbon isotopic fractionation in the biosynthesis of bacterial fatty acids. Ozonolysis of unsaturated fatty acids as a means of determining the intramolecular distribution Ellipsis. *Geochim. Cosmochim. Acta* **46**, 139–149.

Morais E. T. (2007) *Aplicações de técnicas de inteligência artificial para classificação genética de amostras de óleo da porção terrestre, Bacia Potiguar, Brasil* (M.Sc. Dissertation). Federal University of Rio de Janeiro.

Ni Y., Ma Q., Ellis G. S., Dai J., Katz B., Zhang S. and Tang Y. (2011) Fundamental studies on kinetic isotope effect (KIE) of hydrogen isotope fractionation in natural gas systems. *Geochim. Cosmochim. Acta*, 1–12.

Piasecki A., Sessions A. L., Lawson M., Ferreira A. A., Neto E. V. S. and Eiler J. (2016a) Analysis of the site-specific carbon isotope composition of propane by gas source isotope ratio mass spectrometer. *Geochim. Cosmochim. Acta* **188**, 58–72.

Piasecki A., Sessions A. L., Peterson B. and Eiler J. (2016b) Prediction of equilibrium distributions of isotopologues for methane, ethane and propane using density functional theory. *Geochim. Cosmochim. Acta* **190**, 1–12.

Rustad J. R. (2009) Ab initio calculation of the carbon isotope signatures of amino acids. *Org. Geochem.* **40**, 720–723.

Santos Neto dos E. V. and Hayes J. M. (1999) Use of hydrogen and carbon stable isotopes characterizing oils from the Potiguar Basin (onshore), Northeastern Brazil. *Bulletin*.

Schimmelmann A. and Sessions A. L. (2006) Hydrogen isotopic (D/H) composition of organic matter during diagenesis and thermal maturation. *Annu. Rev. Earth Planet. Sci.* **34**, 501–533.

Schimmelmann A., Lewan M. D. and Wintsch R. P. (1999) D/H isotope ratios of kerogen, bitumen, oil, and water in hydrous pyrolysis of source rocks containing kerogen types I, II, IIS, and III. *Geochim. Cosmochim. Acta* **63**, 3751–3766.

Stolper D. A., Lawson M., Davis C. L., Ferreira A. A., Neto E. V. S., Ellis G. S., Lewan M. D., Martini A. M., Tang Y., Schoell M., Sessions A. L. and Eiler J. (2014a) Formation temperatures of thermogenic and biogenic methane. *Science* **344**, 1500–1503.

Stolper D. A., Sessions A. L., Ferreira A. A., Santos Neto E. V., Schimmelmann A., Shusta S. S., Valentine D. L. and Eiler J. (2014b) Combined 13C–D and D-D clumping in methane: Methods and preliminary results. *Geochim. Cosmochim. Acta* **126**, 169–191. https://doi.org/10.1016/j.gca.2013.10.045.

Stolper D. A., Martini A. M., Clog M., Douglas P. M., Shusta S. S., Valentine D. L., Sessions A. L. and Eiler J. (2015) Distinguishing and understanding thermogenic and biogenic sources of methane using multiply substituted isotopologues. *Geochim. Cosmochim. Acta*, 1–61.

Suda K., Gilbert A., Yamada K., Yoshida N. and Ueno Y. (2017) Compound- and position-specific carbon isotopic signatures of abiogenic hydrocarbons from on-land serpentinite-hosted Hakuba Happo hot spring in Japan. *Geochim. Cosmochim. Acta* **206**, 201–215.

Sun X., Zhang T. W., Sun Y. G., Milliken K. L. and Sun D. Y. (2016) Geochemical evidence of organic matter source input and depositional environments in the lower and upper Eagle Ford Formation, south Texas. *Org. Geochem.* **98**, 66–81.

Takenaka S., Kuriyama T., Tanaka T. and Funabiki T. (1995) Photooxidation of propane over alkali-ion-modified V_2O_5/SiO_2 catalysts. *J. Catal.* **155**, 196–203.

Tang Y., Perry J. K., Jenden P. D. and Schoell M. (2000) Mathematical modeling of stable carbon isotope ratios in natural gases. *Geochim. Cosmochim. Acta*.

Tang Y., Huang Y., Ellis G. S., Wang Y., Kralert P. G., Gillaizeau B., Ma Q. and Hwang R. (2005) A kinetic model for thermally induced hydrogen and carbon isotope fractionation of individual n-alkanes in crude oil. *Geochim. Cosmochim. Acta* **69**, 4505–4520.

Toyoda S. and Yoshida N. (1999) Determination of nitrogen isotopomers of nitrous oxide on a modified isotope ratio mass spectrometer. *Anal. Chem.* **71**, 4711–4718.

Trindade L., Brassell S. C. and Neto E. (1992) Petroleum migration and mixing in the Potiguar Basin, Brazil (1). *Bulletin*.

Wang Z., Schauble E. A. and Eiler J. (2004) Equilibrium thermodynamics of multiply substituted isotopologues of molecular gases. *Geochim. Cosmochim. Acta* **68**, 4779–4797. Available at: <http://linkinghub.elsevier.com/retrieve/pii/S001670370400451X>.

Webb M. A. and Miller III T. F. (2014) Position-Specific and clumped stable isotope studies: Comparison of the Urey and Path-Integral approaches for Carbon Dioxide, Nitrous Oxide, Methane, and Propane. *J. Phys. Chem. A* **118**, 467–474.

Zou Y.-R., Cai Y., Zhang C., Zhang X. and Peng P. (2007) Variations of natural gas carbon isotope-type curves and their interpretation – a case study. *Org. Geochem.* **38**, 1398–1415.

Associate editor: Sarah J. Feakins